Solvation of the Halide Anions in Dimethyl Sulfoxide. Factors Involved in Enhanced Reactivity of Negative Ions in Dipolar Aprotic Solvents

Tom F. Magnera, Gary Caldwell, Jan Sunner, Sigeru Ikuta, and Paul Kebarle*

Contribution from the Chemistry Department, University of Alberta, Edmonton, Alberta, Canada T6G 2G2. *Received January 23, 1984*

Abstract: The equilibrium constants $K_{n-1,n}$ for the gas-phase equilibria $(n-1,n)$ $X^-(Me_2SO)_{n-1} + Me_2SO = X^-(Me_2SO)_n$, $X = Cl^-$, Br^-, I^- ($n = 1$ to $n = 3$ or 4) were measured with a pulsed high-pressure mass spectrometer. van't Hoff plots of these data lead to $\Delta H^\circ_{n-1,n}$, $\Delta S^\circ_{n-1,n}$, and $\Delta G^\circ_{n-1,n}$. These data represent information on the inner-shell solvation of X^- to Me_2SO. Comparison with work in the preceding paper, this issue, on $K^+(Me_2SO)_n$ shows that the positive isoelectronic ion K^+ bonds to Me_2SO much more strongly than Cl^-. MO calculations at the 4-31G level for these systems and improved electrostatic calculations are used to show that this is due to electrostatic reasons, i.e., the location of the dipole in Me_2SO is largely on the S^+O^- group. This dipole can be approached easily by K^+ but not by Cl^- since the methyl groups interfere in the latter case. Comparing the inner-shell solvation of Cl^- by Me_2SO and H_2O one finds that, in spite of the above effect, Me_2SO bonds more strongly, a consequence of the much higher dipole moment of Me_2SO. However, in the liquid solvents H_2O provides better solvation. This is a consequence of the much larger radius of the Cl^-Me_2SO inner-shell cluster when compared with the Cl^-, H_2O cluster, i.e., significant solvation beyond the inner shell occurs for Cl^-, H_2O but not for Cl^-Me_2SO. Comparison of the data for Cl^-, Br^-, I^- in Me_2SO and water shows that both the inner-shell solvation and more importantly the solvation in the liquid solvents decreases for Me_2SO and H_2O in the order Cl^-, Br^-, I^-, i.e., with increasing ion size; however, the decrease in the dipolar aprotic solvents is appreciably less. The smaller decrease of solvation with an increase of ion radius is the principal reason for the much higher rates of reactions $A^- + B = (AB^-)^* \rightarrow C^- + D$ in dipolar aprotic solvents. The reaction $Cl^- + CH_3Br = ClCH_3 + Br^-$ is examined in detail on the basis of its reaction coordinate in the gas phase and in solution. It is shown on the basis of sound thermochemical data for the relative solvation energies of X^- that good predictions of the activation energy in protic and aprotic solvents can be made.

Dipolar aprotic solvents like dimethyl sulfoxide (Me_2SO), dimethylformamide (DMF), acetonitrile, and acetone are used extensively in organic synthetic work. Of particular importance is their ability to accelerate reactions involving anionic reactants and transition states. A simple example is the S_N2 reaction 1 which in DMF has a rate that is 10^5 times higher than that in water.[1] The reasons for observing higher rates in dipolar aprotic

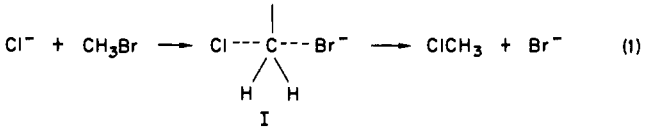

(1)

solvents have been much studied and discussed, and many useful insights have been provided.[2,3] However, this earlier work has also perpetrated some misconceptions that seem still to be widely held. The earlier work did not enjoy the benefit that modern MO computations can provide. Another new area that provides valuable information is the study of ionic reactions in the gas phase. Thus, the study of reaction 1 in the gas phase provides information on the energy of the transition state relative to that of the reactants in the absence of solvent molecules,[4,5] while the determination of ion–solvent molecule equilibria in the gas phase as shown in reactions 2 and 3, where L is a molecule of a given solvent, provides values for $\Delta H^\circ_{n-1,n}$, $\Delta G^\circ_{n-1,n}$, and $\Delta S^\circ_{n-1,n}$ and thus information

$$X^-L_{n-1} + L = X^-L_n \qquad (n-1,n) \qquad (2)$$

$$M^+L_{n-1} + L = M^+L_n \qquad (n-1,n) \qquad (3)$$

on the inner-shell solvation of ions by different solvent molecules. We hope to be able to demonstrate in the present work the usefulness of such information. First we will concentrate on the pertinent ion–solvent molecule interactions and then combine this material with the gas-phase data on reaction 1, to provide a more rigorous interpretation of the factors involved in making the rates of S_N2 reactions like (1) much faster in dipolar aprotic solvents than in protic solvents.

The alkali cations and halide anions are a classical series in ion-solvation studies. These spherically symmetrical closed-shell ions provide the best example for changes of solvation with change of ionic radius and change of sign of the ionic charge. While the dependence on radius cannot be directly used to provide an exact value for the solvation of an ion like the transition state in the S_N2 reaction 1, for which a "correct" radius cannot be assigned, nevertheless semiquantitative values can be obtained on the basis of reasonable estimates of the transition-state ion radius.

Measurements of the clustering equilibria 2 and 3 for the halide and alkali ions and the protic solvent water[6] and the dipolar aprotic solvent acetonitrile[7] have already been reported. In the present work we provide results for X^- (Cl^-, Br^-, I^-) and Me_2SO. These will be compared first with the solvation for the positive ions by Me_2SO see preceding paper in this issue,[8] and then a comparison of X^- solvation by H_2O and the aprotic Me_2SO and acetonitrile will be made. The insights gained will be used to analyze the causes for the rate differences of reaction 1 observed in protic and aprotic solvents.

Experimental Section

The measurements were performed with a pulsed electron beam high pressure mass spectrometer. The same instrument was used as that employed in earlier studies of X^- and acetonitrile[6] and the kinetics of the S_N2 reaction.[5]

A mixture containing methane was used as the major (bath) gas, and Me_2SO was passed through the ion source at pressures in the 1–6-torr range. Typically the partial pressures of Me_2SO were between 1 and 10 mtorr. The negative ions X^- were produced by adding traces of suitable compounds to the reaction mixture. Cl^- was produced from CCl_4, Br^- from CH_2Br_2, and I^- from CH_3I. These compounds engage in dissociative electron capture as illustrated for CCl_4: $CCl_4 + e = Cl^- + CCl_3$.

(1) Bathgate, R. H.; Moelwyn-Hughes, E. A. *J. Chem. Soc.* **1959**, 2642.
(2) Parker, A. J. *Q. Rev., Chem. Soc.* **1962**, *16*, 163.
(3) Parker, A. J. *Chem. Rev.* **1964**, *69*, 1.
(4) Farneth, W. E.; Brauman, J. I. *J. Am. Chem. Soc.* **1976**, *98*, 5546. Olmstead, W. N.; Brauman, J. I. *J. Am. Chem. Soc.* **1977**, *99*, 4219.
(5) Caldwell, G.; Magnera, T. F.; Kebarle, P. *J. Am. Chem. Soc.* **1984**, *106*, 959.
(6) Arshadi, M.; Yamdagni, R.; Kebarle, P. *J. Phys. Chem.* **1970**, *74*, 1475.
(7) Davidson, W. R.; Kebarle, P. *J. Am. Chem. Soc.* **1976**, *98*, 6125. Yamdagni, R.; Kebarle, P. *J. Am. Chem. Soc.* **1972**, *94*, 2940.
(8) Sunner, J.; Kebarle, P. *J. Am. Chem. Soc*, preceding paper in this issue.

0002-7863/84/1506-6140$01.50/0

Table I.[a] Thermochemistry of Clustering Reactions $(n-1,n)$ $X^-L_{n-1} + L = X^-L_n$ from Gas-Phase Equilibria, L = Me_2SO and H_2O and X^- = Cl^-, Br^-, and I^-

	H_2O[b]									Me_2SO[c]								
	Cl^-			Br^-			I^-			Cl^-			Br^-			I^-		
$(n-1,n)$	ΔH	ΔG	ΔS	ΔH	ΔG	ΔS	ΔH	ΔG	ΔS	ΔH	ΔG	ΔS	ΔH	ΔG	ΔS	ΔH	ΔG	ΔS
0,1	13.1	8.2	16.5	12.6	7.1	18.4	10.3	5.4	16.3	18.6	12.5	20.4	17.3	10.9	21.4	15.7	9.2	21.7
1,2	12.7	6.5	20.8	12.3	5.4	22.9	9.8	4.1	19.0	16.0	8.9	23.8	14.5	7.8	22.4	12.8	6.2	22.0
2,3	11.7	4.5	23.2	11.5	4.1	24.8	9.4	3.0	21.3	14.9	6.0	29.8	13.6	5.3	27.5	11.6	4.1	25.1
3,4	11.7	3.4	25.8	10.9	2.9	26.8				14.6	3.5	37.2						
4,5										13.8	1.8	40.2						

[a] $\Delta H°$ and $\Delta G°$ in kcal/mol. $\Delta S°$ in cal deg^{-1} mol^{-1}. Standard state 1 atm. [b] From ref 6. [c] Present work.

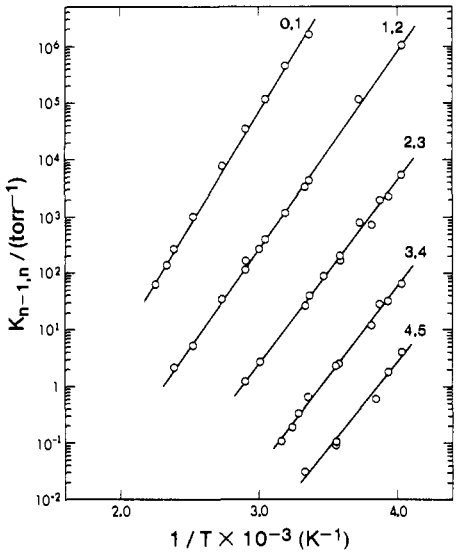

Figure 1. van't Hoff plots of equilibrium constants $K_{n-1,n}$ for reactions $Cl^-(Me_2SO)_{n-1} + Me_2SO = Cl^-(Me_2SO)_n$.

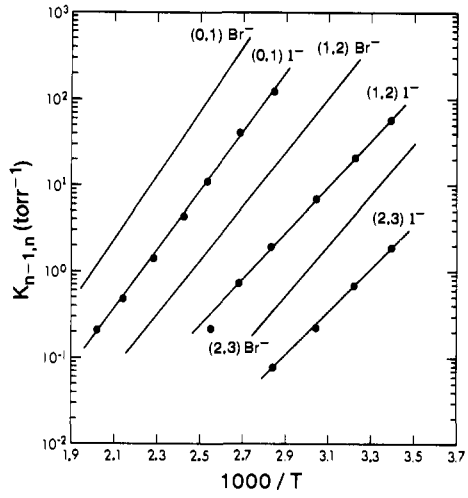

Figure 2. van't Hoff plots of equilibrium constants $K_{n-1,n}$ for $Br^-(Me_2SO)_{n-1} + Me_2SO = Br^-(Me_2SO)_n$ and $I^-(Me_2SO)_{n-1} + Me_2SO = I^-(Me_2SO)_n$.

The dissociative electron capture reactions are exothermic and have unusually large rate constants, $k \gg 10^{-9}$ molecules^{-1} cm^3 s^{-1}, such that only traces of the electron capture agents need to be used.

Results and Discussion

A. Comparison between Positive and Negative Ions in the Gas Phase and Solution, Me_2SO and H_2O. The van't Hoff plots observed for the equilibria involving Cl^-, Br^-, I^-, and Me_2SO are shown in Figures 1 and 2. The $\Delta H°$, $\Delta G°$, and $\Delta S°$ values obtained from the van't Hoff plots are given in Table I.

The enthalpy changes for the clustering of Cl^- with Me_2SO are compared with the corresponding changes for the isoelectronic positive ion K^+ and Me_2SO in Figure 3, while Figure 4 gives the same comparison but for the free energy changes. A very much

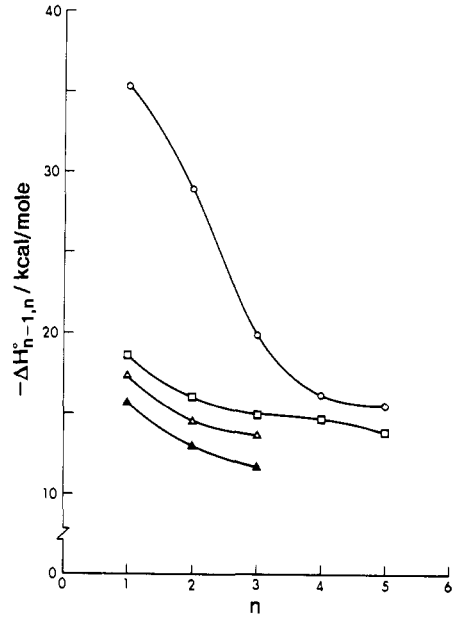

Figure 3. Comparison of $\Delta H°_{n-1,n}$ changes for clustering of K^+ (○), Cl^- (□), Br^- (△), and I^- (▲) with Me_2SO. The binding of Me_2SO to K^+ is very much stronger than that to the isoelectronic Cl^-; however, the stepwise bonding of Me_2SO molecules becomes nearly the same for the isoelectronic pair at high n. The decreasing bonding of X^- to Me_2SO is observed in the order Cl^-, Br^-, I^-. This order is opposite to the order I^-, Br^-, Cl^- often quoted in the literature and believed to be due to strong polarizability interactions between the large I^- and the large dipolar aprotic solvent molecule: (○) K^+, (□) Cl^-, (△) Br^-, (▲) I^-.

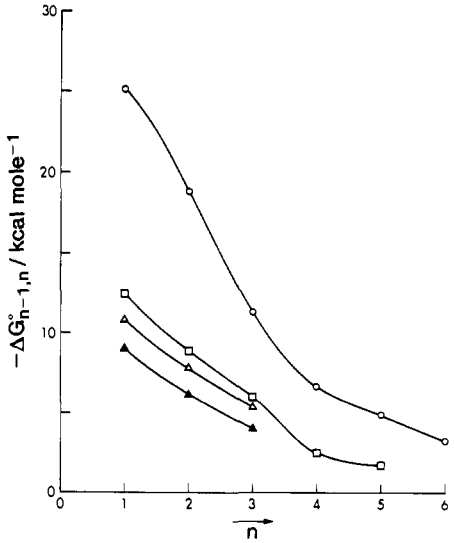

Figure 4. Comparison of free energy changes $\Delta G°_{n-1,n}$ for K^+, Cl^-, Br^-, I. Remarks given in Figure 3 for the bonding enthalpies apply also to the bonding free energies: (○) K^+, (□) Cl^-, (△) Br^-, (▲) I^-.

stronger bonding to the positive ion is observed in both figures. The differences are largest for the (0,1) interactions and decrease with an increase of n. Thus $-\Delta H_{0,1}$ for K^+ is almost twice as large

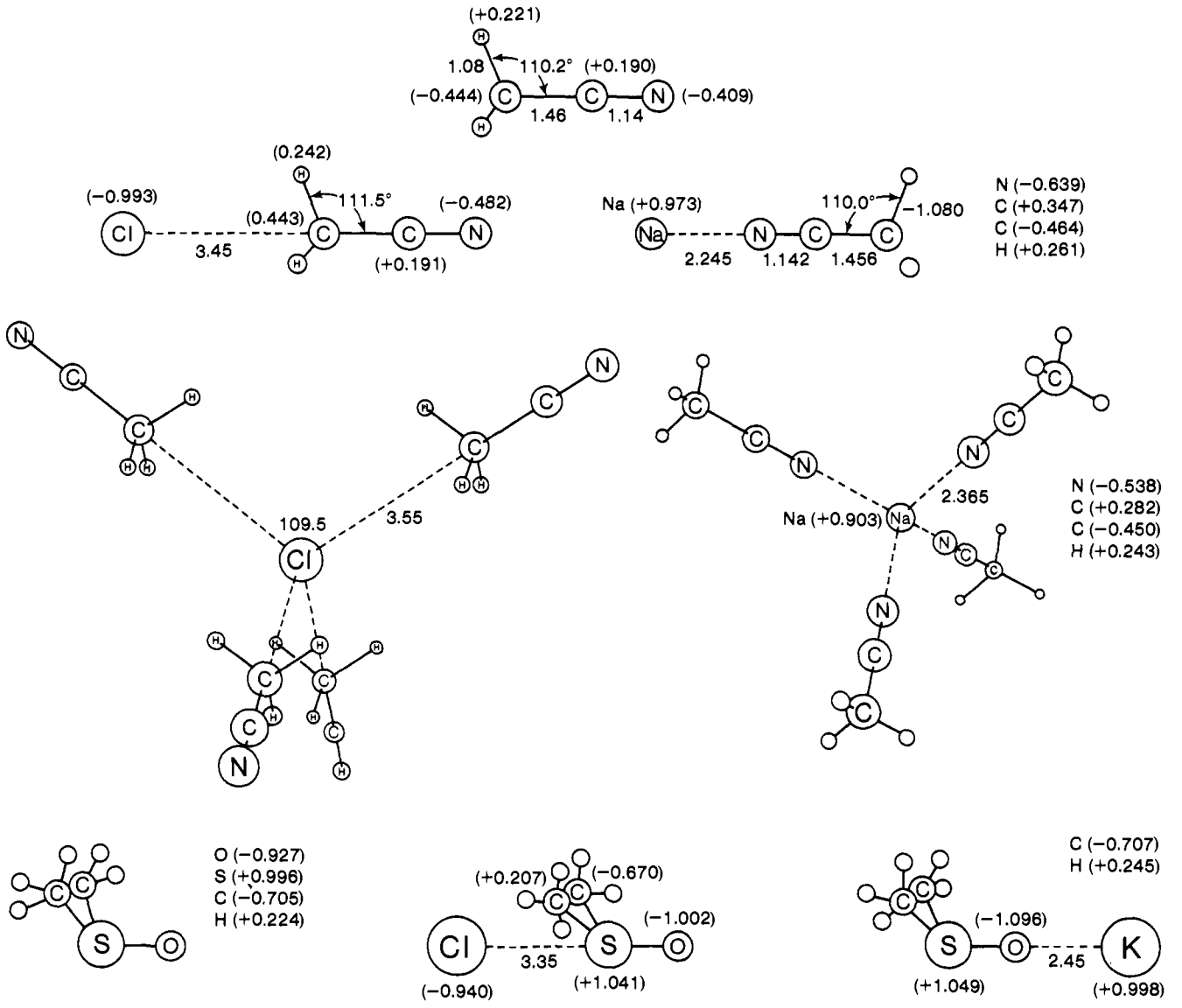

Figure 5. Structures for Na^+MeCN and Cl^-MeCN clusters obtained from SCF computations by Yamabe and Hirao.[10] Net atomic charges based on Mulliken electron populations are given in parentheses. Interatomic distances are angstroms. Calculations for K^+Me_2SO and Cl^-Me_2SO are from the present work. Observed very small changes in net atomic charge of ion before and after clustering show that very little electron transfer occurs and bonding is essentially electrostatic. Computed binding energies of clusters are given in Table I and Table III. These show that the negative isoelectronic ion bonds much more weakly to the dipolar aprotic molecule than the positive ion.

as that for Cl^-, while the $-\Delta H_{3,4}$ for the two ions are almost the same (Figure 3). Stronger bonding for the positive isoelectronic ion was observed also in our earlier study of the alkali and halide ions and acetonitrile.[7] Since the bonding is dominated by electrostatic terms, i.e., the ion–dipole and the ion–induced dipole attraction between the ion and the molecule, the large difference between the positive and negative ion was explained[7] as being a consequence of the net atomic charge distribution and the atomic or bond polarizability distribution in acetonitrile. Most of the dipole and most of the polarizability are located on the C≡N group, and this group can be easily approached by the positive ion in an attractive interaction with the dipole. On the other hand, the negative ion cannot come close to the positive end of the $N^-\equiv C^+$ dipole because of steric interference by the methyl group. A later, theoretical study by Hirao and Yamabe[9] utilizing the 4-31G basis set for the calculation of $Li^+(CH_3CN)_n$, $Na^+(CH_3CN)_n$, $F^-(CH_3CN)_n$, and $Cl^-(CH_3CN)_n$ has confirmed these findings and interpretation. Table II gives a comparison between the experimental $\Delta H^\circ_{n-1,n}$ values[7] and the theoretical $\Delta E_{n-1,n}$ binding energies of these authors.[9] Looking at the isoelectronic Na^+ and F^- one finds that both the experimental and theoretical results predict a nearly twice higher binding energy for the positive ion. Some of the structures obtained by Hirao and Yamabe are shown in Figure 5.

Table II. Experimental and Theoretical Binding Energies[a] for $(n-1, n)$ Reactions $X^-L_{n-1} + L = X^-L_n$ and $M^+L_{n-1} + L = M^+L$

	Na^+MeCN		F^-MeCN		K^+MeCN	Cl^-MeCN	
$(n-1,n)$	$-\Delta E^b$	$-\Delta H^c$	$-\Delta E^b$	$-\Delta H^c$	$-\Delta H^c$	$-\Delta E^b$	$-\Delta H^c$
0,1	35.8	32	18.2	16.0	24.4	11.5	13.4
1,2	30.5	24.4	15.5	12.9	20.6	10.3	12.2
2,3	22.8	20.6	13.6	11.7	18.2	8.9	10.6
3,4	16.6	14.9	9.3	10.4	14.6	7.2	6.2

	K^+Me_2SO		Cl^-Me_2SO	
0,1	ΔE^d	ΔH^e	ΔE^d	ΔH^d
0,1	39.6	34.5	21.0	18.6

[a] All values in kcal/mol. [b] From Hirao[9,10]. [c] From Kebarle.[7] [d] Present work. [e] From Sunner.[8]

We have performed theoretical calculations for Cl^-Me_2SO and K^+Me_2SO. The 4-31G basis set was used for Me_2SO and Cl^-[10]

(9) Yamabe, S.; Hirao, K. *Chem. Phys. Lett.* **1981**, *84*, 598. Hirao, K.; Yamabe, S.; Sano, M. *J. Phys. Chem.* **1982**, *86*, 2626.

(10) King, H.; Dupuis, M.; Rys, J. Nat. Resource Comput. Chemistry Software Cat. Vol. 1, PROG. NO 2H02 (HONDO 5), 1980, Lawrence Berkeley Laboratory, University of California.

Table III. Results[a] from Electrostatic Calculations for K^+Me_2SO and Cl^-Me_2SO

	E_{DIP}	E_{POL}[c]	E_{DIS}[c]	E_{rep}[b]	E	$\Delta H_{0,1}$[d]
K^+Me_2SO	−28.9	−6.2	−1.4	+7.7	−28.8	−34.5
Cl^-Me_2SO	−13.7	−11.9	−4.5	+9.8	−21	−18.6

[a] All values in kcal/mol, see eq 4. [b] E_{rep} was evaluated with $E_{rep} = C\exp(-Ar_{ij})$ where $C = C_iC_j^{1/2}$ and $A = (A_i + A_j)/2$. The values for $C \times 10^{-3}$ (kcal/mol) were $K^+ = Cl^- =$ S, 225; O, 18.7; C, 3.66; H, 0.696 for A and $K^+ = Cl^-$ = S, 3.26; O, 3.565; C, 2.753; H, 3.01 ($Å^{-1}$), see ref 7, 12, 13. [c] The larger $-E_{POL}$ and $-E_{DIS}$ for Cl^-Me_2SO relative to K^+Me_2SO are mostly due to the presence of the S atom near Cl^-. The S atom is much more polarizable than the O atom which is nearest to K^+ in K^+Me_2SO. [d] Experimental results from Tables I and II.

while a basis set due to Huzinaga[11] was used for K^+. The results are summarized in Table II and Figure 5. The most stable structures given in Figure 5 show that the positive and the negative ions line up with the S=O bond dipole axis. The approach of K^+ to the negative end of the dipole is unhindered, while Cl^- is prevented from coming close by the presence of the two methyl groups. The calculation predicts a much higher binding energy for the positive ion in agreement with experiment. The net atomic charges obtained from the Mulliken populations are given in Figure 5. These show that only 0.002 e is transferred to K^+ on formation of the complex. The electron transfer from Cl^- to Me_2SO is somewhat larger (0.060 e) but still quite small. The bonding in both cases is largely electrostatic. The polarization of the Me_2SO and particularly the SO group is clearly indicated by the increase of opposite sign charges on the S and O atoms after formation of the complex.

Improved electrostatic calculations[7,12,13] of the interaction (bond) energy of the complexes $K^+(Me_2SO)$ and $Cl^-(Me_2SO)$ provide useful qualitative insights. The energy of interaction E was obtained from eq 4 where the successive terms stand for ion–dipole, ion–induced dipole, ion–molecule dispersion attraction, and ion–molecule repulsive interactions. The equations used for the

$$E = E_{DIP} + E_{POL} + E_{DIS} + E_{REP} \quad (4)$$

evaluation of the individual terms are given in Davidson[7] and Sunner.[13] The E_{DIP} term was evaluated by summing over the Coulombic interactions of the ion with the net atomic charges of the Me_2SO molecule.[14] The results obtained are given in Table III. The predicted binding energy for $K^+(Me_2SO)$ ($-E$ = 29 kcal/mol) is considerably larger than that for $Cl^-(Me_2SO)$ ($-E$ = 21 kcal/mol), in agreement with experiment and the quantum mechanical calculations. The dominant term is $-E_{DIP}$ which for K^+ is twice as large as for Cl^-, a consequence of the close approach that K^+ can make to the SO bond dipole.

The binding energies for $X^-(Me_2SO)_n$ are compared with those for $X^-(H_2O)_n$ in Table I. One finds both the $-\Delta H^\circ_{n-1,n}$ and $-\Delta G^\circ_{n-1,n}$ for Me_2SO to be larger than those for H_2O. This result may appear surprising at first glance, since the evidence above showed that the bonding of Me_2SO to X^- is weakened by the interference of the methyl groups. However, the dipole moment of Me_2SO is 4.1 D while that for H_2O is only 1.8 D. Also the approach of X^- to the S=O group is not completely barred, due to the pyramidal structure of the Me_2SO molecule (see Figure 5) which keeps the methyl groups partially out of the way. Evidently, these two factors and the higher polarizability of Me_2SO produce the stronger interactions for Me_2SO. Acetonitrile, which has a similar dipole (3.9 D) but in which the methyl group interferes very effectively (see Figure 5), leads to bonding with X^- which is appreciably weaker than that for Me_2SO and thus closer to the bonding with H_2O.[7]

Table IV. Results from Calculations[a] for the Cycle in Eq 5 for the Single-Ion Solvation Free Energy of K^+ and Cl^-: $\Delta G^\circ_S(K^+)$ and $\Delta G^\circ_S(Cl^-)$ in Liquid Me_2SO and H_2O

ion	solvent	$-\Delta G^\circ_{0,4}$	r_i[b]	$-\Delta G^\circ_i$	$-\Delta G^\circ_{Born}$	ΔG°_{cav}	$-\Delta G^\circ_P$
K^+	H_2O	31.0	4.6 (4.2)	22.8	35.2	27.5	30.5
K^+	Me_2SO	62	6.3 (6.1)	45.6	25.7	30.8	41
Cl^-	H_2O	22.8	4.6	14.6	35.2	27.5	22
Cl^-	Me_2SO	31.4	6.3	15.0	25.7	30.8	10

[a] All energy values in kcal/mol. For equations defining individual terms see eq 5–10. [b] Radius of inner-shell cluster. Values in parentheses were evaluated for the K^+ clusters; values not in parentheses were evaluated for the Cl^- clusters. In order not to bias the calculation the same r were used for K^+ and Cl^- clusters.

The gas-phase data (Table I) can be used in a Born-type cycle to obtain insights into the ion solvation in the liquid protic and aprotic solvents. Starting with the naked gas-phase ion X^- and the liquid solvent $L_{(l)}$, we evaporate i molecules of the solvent and add them to X^- forming $X^-(L)_i$ in the gas phase. The free energy for this step is

$$\Delta G^\circ_i = \Delta G^\circ_{0,i}(X^-) - i\Delta G_{vap}(L)$$

Then a cavity that can accommodate the inner-shell cluster is made in the solvent. The endothermic free energy required for this step is ΔG°_{cav}. The inner-shell cluster is then put in the cavity of the solvent. The energy released is the Born charging solvation term of the inner cluster ΔG°_{Born} and ΔG°_{inter} a term due to intermolecular bonding between the solvent molecules of the cluster and the solvent molecules forming the surface of the cavity. The terms and the equations used for their evaluation are given in eq 5–10 written for a negative ion X^- and solvent L.

$$\Delta G^\circ_{solv}(X^-) = \Delta G^\circ_{0,i} - i\Delta G_{vap}(L) + \Delta G^\circ_{cav} + \Delta G^\circ_{Born} + \Delta G^\circ_{inter} \quad (5)$$

$$\Delta G^\circ_{0,i} = \Delta G^\circ_{0,1} + \Delta G^\circ_{1,2} \ldots + \Delta G^\circ_{i-1,i} \quad (6)$$

from gas-phase equilibria

$$\Delta G^\circ_{vap}(L) = RT \ln 1/P^\circ_L \quad (7)$$

P° = vapor pressure of L(atm) at T = 300

$$\Delta G^\circ_{cav} = 4\pi r^2\sigma_L \quad (8)$$

r = radius of the inner-shell cluster; σ_L = surface tension of liquid L

$$\sigma(H_2O) = 72;\ \sigma(Me_2SO) = 43 \text{ (cgs)}$$

$$\Delta G^\circ_{Born} = \frac{-z^2e^2}{8\pi\epsilon_0 r}\left(1 - \frac{1}{D_L}\right) = \frac{165.2}{r\ (Å)}\left(1 - \frac{1}{D_L}\right) \text{ (kcal/mol)} \quad (9)$$

D_L = dielectric constant of liquid L; $D_{H_2O} = 80$; $D_{Me_2SO} = 46.4$

$$\Delta G^\circ_{inter} \approx i(0.5\Delta H_{vap}(L)) \quad (10)$$

The radius of the cluster r was assumed equal to the radius of the cavity. The radii used[16–18] are given in Table IV. For the

(11) Huzinaga, S. Chemistry Department, University of Alberta, Edmonton, Canada T6G 2G2.

(12) Eliezer, I.; Krindel *J. Chem. Phys.* **1972**, *57*, 1884. Spears, K. *J. Chem. Phys.* **1972**, *51*, 1850, 1884.

(13) Sunner, J.; Nishizawa, K.; Kebarle, P. *J. Phys. Chem.* **1981**, *89*, 1011.

(14) The net atomic charges from the 4-31G MO calculation lead to a Me_2SO dipole of 6.87 D while the experimental dipole is 4.1 D. Therefore the net atomic charges used in the electrostatic calculations were scaled down by multiplying with the factor 4.1/6.87. It should be noted that the ΔE binding energies from the MO calculations (Table II) do not depend on the accuracy of the Me_2SO dipole evaluated from the net atomic charges. The latter are obtained from Mulliken electron populations and are strongly basis set dependent.

(15) Saluja, P. P. S. *MTP Int. Rev. Sci.: Phys. Chem. Ser. Two* **1976**, *6*, 1.

(16) The values of the cluster radius $K(H_2O)$ can be evaluated from $r(K^+H_2O) = r(K^+–O) + r(OH) + r(H) = 2.7 + 1 + 1 \approx 4.7$ Å where $r(K^+–O)$ is Clementi's[17] value for the K^+OH_2 species. Proceeding in a similar manner and using Clementi's value for $r(Cl^-H_2O)$ and the calculated values for $r(K^+–Me_2SO)$ and $r(Cl^–Me_2SO)$ of the present work and the known dimensions of the Me_2SO molecule,[18] one can evaluate values for the K^+ clusters given in parentheses in Table IV. Since the K^+ and Cl^- values are close, we have adopted the Cl^- values also for the K^+ clusters.

number of the inner-shell ligands we have used $i = 4$, since the gas-phase data do not extent to higher i. The term $\Delta G°_i = \Delta G°_{0,i} - i\Delta G°_{vap}$ is quite insensitive to the value of i in the range 4–6 because $\Delta G_{i-1,i} \approx \Delta G_{vap}$ (in the range i equals 4–6) such that a cancellation occurs. The term $\Delta G°_{inter}$ is probably proportional to i. We have not evaluated this term since rather arbitrary assumptions must be made. Probably a value of $i = 6$ should be used for that term. The partial sum of all the terms except $\Delta G°_{inter}$ is given in Table IV as $\Delta G°_P$. Accurate evaluations of $\Delta G°_{solv}$ cannot be expected from the cycle in eq 5 and the equations used. A discussion of this cycle and the problems involved is given by Saluja.[15] We will restrict ourselves in utilizing the results only to uncover those gross effects, which can be expected to be well accounted for by the cycle in eq 5 and eq 5–10.

The $\Delta G°_{cav}$ terms for the K^+ and Cl^- clusters are expected to be very close since the radii of the two clusters are very similar.[16] The $\Delta G°_{cav}$ terms for the H_2O- and Me_2SO-containing clusters turn out to be also approximately the same (Table IV). While the radius of the Me_2SO clusters is considerably larger, the surface tension of Me_2SO is smaller, such that a compensation occurs. Thus the relative ΔG_P are dominated by the gas-phase $\Delta G°_i$ and the Born $\Delta G°_{Born}$ terms. The $-\Delta G°_{Born}$ terms for Me_2SO are 10 kcal/mol smaller than for H_2O. This important difference is a consequence of the larger radius of the Me_2SO inner-shell cluster. The dielectric constants of Me_2SO and water are also different, but the Born energy is very unsensitive to the values of D_L when these are large (see eq 8).

Examining first K^+ in H_2O and Me_2SO we find that the $-\Delta G°_{0,4}$ term for Me_2SO is larger by 31 kcal/mol. At the $\Delta G°_i$ level, due to the higher vaporization energy of Me_2SO, this difference is reduced to 23 kcal/mol and at the $\Delta G°_P$ level the difference is reduced to 10 kcal/mol, mainly due to the much less exothermic Born term for Me_2SO (Table IV).

For Cl^- in H_2O and Me_2SO the changes from term to term are very similar to those for K^+, but the difference in the initial terms $\Delta G°_{0,4}$ is much smaller, i.e., only 9 kcal/mol in favor of Me_2SO (compared with 31 for K^+). Therefore a reversal occurs at the $\Delta G°_P$ level with Cl^- solvated better by 12 kcal/mol in H_2O than in Me_2SO.

Assuming that the $\Delta G°_{inter}$ for all four cases in Table IV are similar, the $\Delta G_P(K^+Me_2SO) - \Delta G_P(K^+H_2O) = -10$ kcal/mol should give the free energy of transfer of K^+ from H_2O to Me_2SO. The corresponding ΔG_P difference for Cl^- is +12 kcal/mol. These values are in qualitative agreement with the free energies of transfer −3 kcal/mol for K^+ and +9 kcal/mol for Cl^- quoted by Cox.[19] The latter are based on experimental free energies of solution of MX salts in H_2O and Me_2SO and the extrathermodynamic assumption that Ph_4As^+ and Ph_4B^- have the same free energies of transfer to Me_2SO.

B. Solvation of Negative Ions X^- in Me_2SO and Water. The gas-phase clustering results for Cl^-, Br^-, I^-, and Me_2SO, Figures 3 and 4, show that the bonding to Me_2SO decreases in the order Cl^-, Br^-, I^-, i.e., with increasing ion radius. The same trend with radius was observed in the earlier work for X^- and acetonitrile[7] and X^- and H_2O.[6] Thus the inner-shell solvation decreases with an increase of the negative ion radius for both protic and aprotic solvents. A comparison between the solvation energies in the gas-phase and the solvation energies in the liquid solvents is given in Figure 6 where the differences of solvation energies for Cl^- and I^- are plotted for H_2O and Me_2SO. Examining first the gas-phase results, we notice that the $\Delta\Delta H_{0,3} = \Delta H_{0,3}(Cl^-) - \Delta H_{0,3}(I^-)$ values for H_2O and Me_2SO are approximately the same. This near equality is apparently the result of the opposing effect of two factors. We saw earlier that the interference of the methyl groups in Cl^-Me_2SO causes the distance between Cl^- and $S^+{=}O^-$ dipole to be large. Due to this effect, the increase of the X^- radius from Cl^- to I^- should have a lesser effect on X^-Me_2SO than on X^-H_2O

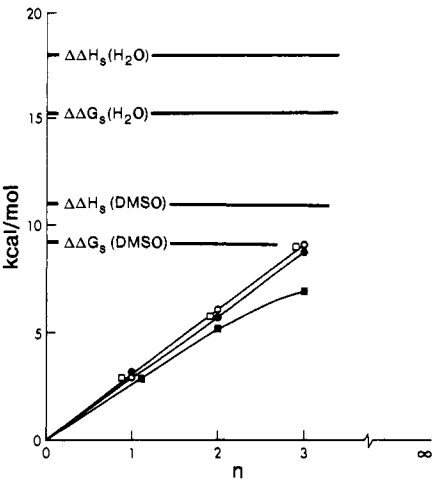

Figure 6. Plot of $\Delta\Delta H°_n = \Delta H°_{0,n}(I^-) - \Delta H°_{0,n}(Cl^-)$ for H_2O and Me_2SO and $\Delta\Delta G°_n = \Delta G°_{0,n}(I^-) - \Delta G°_{0,n}(Cl^-)$ for H_2O and Me_2SO vs. n. Data from Table I. Also given are $\Delta\Delta H°_S = \Delta H°_S(I^-) - \Delta H°_S(Cl^-)$ and $\Delta\Delta G°_S$ for solvation in the liquid solvents H_2O and Me_2SO. Data from Table V. $\Delta\Delta(n)$ data should become equal to $\Delta\Delta(S)$ for $n \to \infty$. For Me_2SO $\Delta\Delta(3)$ approach already $\Delta\Delta(S)$ at $n = 3$. This is not the case for H_2O. $\Delta\Delta H°_n$ H_2O (□); Me_2SO (○); $\Delta\Delta G°_n$ H_2O (■); Me_2SO (●).

where the H_2O dipole can approach X^- closely. However, the dipole moment of Me_2SO is much larger than that of H_2O, and this factor acts in an opposite direction by increasing the absolute magnitude of the X^-Me_2SO bonding and thus also the magnitude of the decrease with an increase of radius from Cl^- to I^-.

The liquid solvent results (Figure 6) show that solvation decreases from Cl^- to I^- for both solvents but much more so for the protic H_2O than the aprotic Me_2SO. Since the inner-shell $\Delta\Delta H_{0,3}$ terms for the two solvents are almost the same, the greater decrease of solvation with an increase of ion radius observed for the (liquid) protic solvent must be mostly due to solvation past the first shell. This deduction from the data in Figure 6 is in line with the calculations summarized in Table IV. These showed that due to the smallness of the inner-shell water cluster $X^-(H_2O)_i$, the Born solvation term of that cluster is large, while for the large Me_2SO inner-shell cluster, the Born solvation term was small. Clearly the bigger decrease of solvation (in the liquid solvent) with an increase of X^- radius in water follows from the importance of the radius-dependent inner-shell Born solvation term for water. The Born term for Me_2SO is small because the Me_2SO molecule is large. Thus solvation of negative ions by dipolar aprotic solvents decreases more slowly with an increase of ion radius because of the unfavorable location of the dipole in the solvent molecules and more importantly because of the large size of the solvent molecules. This large size makes solvation past the inner shell relatively unimportant.

C. Effect of Protic and Aprotic Solvents on Rate of Reactions Involving Negative Ions. The energy dependence of the reaction coordinate for reaction 1, $Cl^- + CH_3Br = ClCH_3 + Br^-$, is shown in Figure 7. The reaction coordinate in the gas phase is based on recent kinetic measurements of the temperature dependence of reaction 1 in the gas phase[5] and theoretical interpretation.[4,5] It will be noted that the energy of the transition state $(Cl\cdots CH_3\cdots Br)^-$ is slightly *lower* than that of the reactants. Thus, the observed activation energy in solution is entirely due to changes of solvation, i.e., due to the energy difference between the solvation of Cl^- and CH_3Br and the less favorable solvation of the transition-state $(ClCH_3Br)^-$. Since the solvation energy of CH_3Br is small compared to that of the ions, the activation energy arises primarily from the solvation energy difference between the small Cl^- and the big transition state. The relationships shown in Figure 7 lead to expression 11 for the activation energy in solution E_A.

$$E_A = \Delta E^*_0 + \Delta H°_S(ClCH_3Br^*) - \Delta H°_S(Cl^-) - \Delta H_S(CH_3Br) \quad (11)$$

Data for the $\Delta H_S(CH_3Br)$ in different solvents are available[20]

(17) Kistenmacher, H.; Popkie, H.; Clementi, E. *J. Chem. Phys.* **1973**, *58*, 1689.
(18) Jacob, W. W., Ed. "Dimethyl Sulfoxide"; Marcel Dekker: New York, 1971; p 3.
(19) Cox, B. G. *Annu. Rep. Prog. Chem., Sect. A* **1973**, *70*, 249.

Table V. Literature Data for Relative Single-Ion Solvation Energies[a] of Halide Ions: $\Delta\Delta H°_S(X^-) = \Delta H°_S(X^-) - \Delta H°_S(Dcl^-)$ and Corresponding $\Delta\Delta G°_S$

	H_2O(l)		HCOOH	MeOH	MeCN	DMF	DMSO	
	$\Delta\Delta H^b$	$\Delta\Delta G^c$	$\Delta\Delta G^d$	$\Delta\Delta H^e$	$\Delta\Delta G_d$	$\Delta\Delta H_e$	$\Delta\Delta H^e$	$\Delta\Delta G_d$
Br^-	8	5	9.6	6.6	1.5	3.3	4.2	4.2
I^-	18	15	18	15.8	6.5	8.9	10.3	6.1

[a] All energy values in kcal/mol. Where only $\Delta\Delta H$ or $\Delta\Delta G$ is given means that another value was not available. [b] Morris.[21] [c] Average of Noyes[22] and Desnoyer.[22] [d] Padova, Table 8.[23] [e] Lattice energies of Morris[21] and $\Delta H_{solution}$ of MX salt, Table 4, Cox.[19]

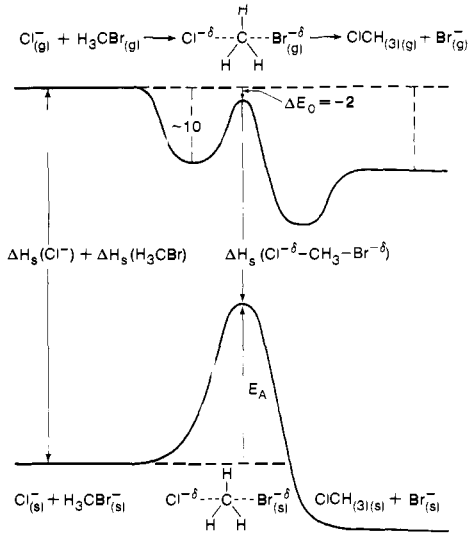

Figure 7. Reaction coordinate for the S_N2 reaction in the gas phase and in solution. ΔH_S are solvation enthalpies of corresponding species and E_A is the experimentally observed activation energy in solution. E_A is entirely due to less favorable solvation of the transition state relative to that of reactants Cl^- and CH_3Br. The situation is typical for many reactions of the type $A^- + B = C^- + D$.

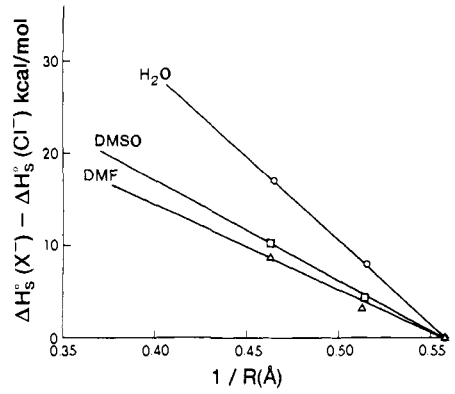

Figure 8. Plot of $\Delta H_S(X^-) - \Delta H_S(Cl^-)$ where $X^- = Br^-$ and I^- vs. reciprocal Pauling radii of respective halide ions. From the data in Table V $\Delta H_S(X^-)$ is the single-ion solvation energy (see Figure 7). The near-linear plot permits extrapolation to larger radii. The transition-state complex $(ClCH_3Br)^-$ may be expected to have a radius larger than that for I^- (2.16 Å). Taking the reasonable value of $R = 2.3$ Å one obtains predictions for the activation energies and rates in H_2O and DMS solution which are in fair agreement with experiment: (○) water, (□) Me_2SO liquid, (△) DMF liquid.

although some of these are approximate; this flaw is not important since the ΔH_S of the neutrals are relatively small. The major task in the evaluation of E_A for different solvents by (11) is to obtain the solvation energies of the charged species, i.e., Cl^- and the transition state.

As a guide to how the solvation energies in these solvents change with radius of the ion we consider available data[21-25] for the solvation of Cl^-, Br^-, I^- in protic and aprotic solvents summarized in Table V. Since the absolute single-ion solvation enthalpies are not known and we are interested only in differences, we have shown the data normalized to $\Delta H_S(Cl^-) = 0$. This means that the data are not dependent on any extrathermodynamic assumptions. The results in Table IV demonstrate that the difference $\Delta\Delta H_S = \Delta H_S(I^-) - \Delta H_S(Cl^-)$ (and the corresponding ΔG difference) is much larger for the protic solvents—H_2O (17.3 kcal/mol), HCOOH (>18 kcal/mol), CH_3OH (16 kcal/mol)—than for the aprotic solvents—DMF (9 kcal/mol), Me_2SO (10 kcal/mol). Assuming for the moment that the transition-state $(ClCH_3Br)^-$ has the same radius as I^-, the above values for H_2O and DMF when substituted in (11) together with $\Delta H_S(CH_3Br) = -6$ kcal/mol in H_2O and −8 kcal/mol in DMF (20) leads to activation energy values for liquid water and DMF. These are $E_A(H_2O) = 21$ kcal/mol and $E_A(DMF) = 15$ kcal/mol. Experimental values reported for the activation energies in these solvents are 25 kcal/mol and 18 kcal/mol,[31] i.e., not too far from the preliminary values above. Better agreement with the experimental E_A is obtained by choosing a transition-state radius of 2.3 Å. The $\Delta H_S(X^-)$ data of Table V for H_2O, Me_2SO, and DMF are plotted in Figure 7 vs. the reciprocal radius of the ion. This plot leads to a nearly linear relationship and permits a linear extrapolation to a larger ion radius. With the radius of 2.3 Å one obtains a solvation enthalpy difference of −11 kcal/mol (DMF) and −22 kcal/mol (H_2O) from Figure 7. These values introduced into eq 11 lead to activation energies E_A of 17 (DMF) and 26 (H_2O) kcal/mol which are rather close to the experimental 18 (DMF) and 25 (H_2O). The pre-exponential factors for the rate constants in solutions of H_2O and DMF are essentially the same[1,3] which means that the successful prediction of the activation energies above is also a successful prediction of the relative rates of (1) in the two different solvents. The choice of $r(ClCH_3Br) = 2.3$ Å was made largely because this radius provides solvation energies which fit the experimental E_A. Arguments can be made[24] suggesting a considerably larger radius. In the absence of a theoretical calculation giving the geometry and charge distribution of the transition state, and the effect of the solvent on that distribution, it appears unproductive to argue in favor of a given radius beyond the point that the choice of 2.3 Å falls within the range of values which can be considered reasonable.

There are some widespread misconceptions in the literature[2,3,24] which we hope the analysis given above and in the preceding section will remove. The first one is that negative ion reactions like the S_N2 reaction 1 are faster in the dipolar aprotic solvent because in dipolar aprotic solvents the larger negative ion (i.e., the transition state) is better solvated than the smaller reagent ion (Cl^- in the present example).[2,3,25] The reaction coordinates in Figure 6 show that this cannot be true. If the transition state was solvated more exothermically than the reactant ion, the reaction would have no activation energy at all in dipolar aprotic solvents, and that is contrary to the experimental findings. It

(20) "Selected Values of Chemical Thermodynamic Properties", US Department of Commerce, 1968;f NBS Technical Note 270-3, p 119. Parker, A. J. *Chem. Rev.* **1969**, *69*, 1.

(21) Morris, D. F. C. In "Structure and Bonding"; Springer-Verlag: New York, 1968; Vol. 4, p 70.

(22) Noyes, R. M. *J. Am. Chem. Soc.* **1962**, *84*, 513; **1964**, *86*, 971.

(23) Padova, J. I. In "Modern Aspects of Electrochemistry"; Conway, B. E., Bockris, J. O'M., Eds.; Butterworths: Washington, DC, 1972; Vol. 7, p 1.

(24) A radius much bigger than 2.3 Å will be predicted if one assumed that in the transition state 0.5 e is on Cl and 0.5 e on Br and that the solvation of Cl^- and the transition state follows a Born equation type dependence, i.e., $-\Delta H_S(X^-) \propto e^2/r$.

(25) Amis, E. S.; Hinton, J. F. "Solvent Effects on Chemical Phenomena"; Academic Press: New York; p 283.

should be noted that the gas-phase reaction coordinate in Figure 6 is a typical reaction coordinate, i.e., gas-phase ion–molecule reaction kinetics studies show that very many reactions of the type $A^- + B \rightarrow C^- + D$ proceed via a transition state whose energy lies *below* that of the reactants. This is a consequence of the attractive interactions between the ion A^- and the molecule B which most often are large enough to compensate the energy increase attendant the formation of the transition state. This is the case for all reported reactions which proceed in the gas phase at collision rates.[4,5,26]

The cause for faster rate in the aprotic solvent was deduced above, it is the lesser sensitivity of the aprotic solvent to the increased size of the transition-state ion, i.e., solvation exothermicity decreases with an increase of ion size in both protic and aprotic solvents but less so for the aprotic solvent.

It is often stated[2,3,25] that the (presumed) stronger interaction of the aprotic solvents with the larger negative ion is due to the large polarizability of the ion and the solvent molecule and the effect of "mutual polarization". The data in Tables I and IV clearly show that the interaction of the larger ion with the aprotic solvent is not stronger but weaker than that with the smaller ion. The analysis above also showed that the lesser sensitivity of the aprotic solvent to an increase of negative ion radius is mostly due to the large size of the aprotic solvent molecule (which makes the inner-shell cluster large). Thus the relationship with the large polarizability of the aprotic molecule is only accidental insofar that large size goes with large polarizability.[27] Finally, the theoretical calculations of the bonding of Cl^- to Me_2SO in Table III clearly show that neither the polarizability nor the dispersion terms are of decisive importance to the bonding of the negative ion with the dipolar aprotic solvent.[27,28]

The very strong interaction of the positive ion (M^+) with aprotic solvents (Tables I, III, and IV) also has synthetic utility in negative ion reactions like eq 1 since it promotes the solubility of the salt MX in the solvent ($X^- = Cl^-$ in eq 1) and by complexing with the ion M^+ it prevents the formation of M^+X^- ion pairs. The formation of an ion pair represents a stabilization of the ion X^- and thus acts to reduce its reactivity.

Registry No. Me_2SO, 67-68-5; CH_3Br, 74-83-9.

(26) Nibering, N. N. M. In "Kinetics of Ion Molecule Reactions"; Ausloos, P., Ed.; Plenum Press: New York, 1979.

(27) The notion that the polarizability is a decisive term in the interaction of large ions with large ligands is a basic part of the Hard and Soft Lewis Acid and Base Theory (HSAB) (Pearson[28]), which is presumed to apply to 1:1 complexes. However, the experimental data on which the theory is based involve complexes in solution. Proper consideration of solvent effects significantly changes some of the rationalizations of HSAB.

(28) Pearson, R. G. "Hard and Soft Acids and Bases"; Dowden, Hutchinson and Ross: 1973.

Gas-Phase Structure of Dimethyl Peroxide

Bernhard Haas and Heinz Oberhammer*

Contribution from the Institut für Physikalische und Theoretische Chemie der Universität Tübingen, 7400 Tübingen, West Germany. *Received January 23, 1984*

Abstract: The geometric structure of dimethyl peroxide, $CH_3O–OCH_3$, was studied by gas electron diffraction. The molecular intensities were analyzed by applying a large amplitude model with a double minimum potential for the O–O torsion. The following geometric parameters for the COOC skeleton were obtained: O–O = 1.457 (12) Å, O–C = 1.420 (7) Å, OOC = 105.2 (5)°, and dihedral angle θ = 119 (10)°. Distances and angles are r_a values, and the dihedral angle corresponds to the minima of the potential function. Experimental uncertainties are based on 3σ values and include systematic errors due to the assumptions for vibrational amplitudes and the analytical expression for the potential function. A planar trans configuration of the COOC skeleton with large-amplitude torsional vibration must be rejected on the basis of the electron-diffraction data.

Molecular structures of peroxides have attracted much interest by experimentalists and theoreticians for the past decades. The structural feature of principal interest is the dihedral angle. For noncyclic peroxides dihedral angles from less than 90° (87.5° in F_2O_2[1]) to 180° have been determined. (In this connection only gas-phase structures are considered, since packing effects and intermolecular interactions may strongly affect this parameter.) This large range for the dihedral angle indicates that this parameter is a delicate balance between two opposing effects: (1) interaction between the oxygen lone pairs which favors a dihedral angle of about 90° (assuming sp hybridization for oxygen) and (2) repulsion between the substituents which tends to increase this angle.

For dimethyl peroxide experimental as well as theoretical studies produce rather controversial results for the dihedral angle. An early electron diffraction analysis by the visual method[2] reports an average value for the O–O and C–O bond lengths and the OOC angle, but no value for the dihedral angle. Two PES investigations interprete the splitting of the oxygen lone pair ionization potentials in terms of an exactly planar (θ = 180°) or nearly planar (θ = 170°) trans configuration. In the first study[3] the interpretation of the PES data is based on CNDO/2 calculations which predict a planar trans configuration, whereas in the latter study[4] the energy splitting of the lone pair orbitals is compared to those of other peroxides. Analysis of the IR and Raman spectra[5] and a normal coordinate analysis based on these data,[6] however, reject a planar trans (D_{2h} symmetry) or cis (C_{2v} symmetry) configuration and indicate C_2 symmetry. Microwave spectra for dimethyl peroxide have been recorded,[7,8] demonstrating a nonzero dipole moment, excluding a planar trans configuration. So far, these spectra have not been assigned. Semiempirical and ab initio molecular orbital calculations predict dihedral angles for dimethyl peroxide ranging from 96.5° (MINDO/2[9]) to 180° (CNDO/2[3] and ab initio[10]). The MINDO/3 method (110.7°[11]) and ab initio calculations with

(1) Jackson, R. H. *J. Chem. Soc.* **1962**, 4585–4592.
(2) Allen, P. W.; Sutton, L. E. *Acta Crystallogr.* **1950**, *3*, 46–72.
(3) Kimura, K.; Osafune, K. *Bull. Chem. Soc. Jpn.* **1975**, *48*, 2421–2427.
(4) Rademacher, P.; Elling, W. *Liebigs Ann. Chem.* **1979**, 1473–1482.
(5) Christe, K. O. *Spectrochim. Acta, Part A* **1971**, *27A*, 463–472.
(6) Butwill Bell, M. E.; Laane, J. *Spectrochim. Acta, Part A* **1972**, *28A*, 2239–2245.
(7) Sutter, D., private communication.
(8) Bauder, A., private communication.
(9) Ohkuba, K.; Fujita, T.; Sato, H. *J. Mol. Struct.* **1977**, *36*, 101–110.
(10) Bair, R. A.; Goddard, W. A., III *J. Am. Chem. Soc.* **1982**, *104*, 2719–2724.

0002-7863/84/1506-6146$01.50/0